Behaviour of Bonded CFRP - Concrete Interfaces at Elevated Temperatures

Rodrigo Cordeniz Ferreira

Extended abstract

Master's Degree in Civil Engineering

Jury

President: Prof. Doutor José Joaquim Costa Branco de Oliveira Pedro

Supervisor: Prof. Doutor Eduardo Nuno Brito Santos Júlio

Vowel: Doutor João Pedro Lage da Costa Firmo

October 2015

Behaviour of CFRP-to-Adhesive-to-Concrete Interfaces at Elevated Temperatures

Extended Abstract

1- Introduction

The reinforcement system with reinforced polymers with fibers (FRP) bonded with resin to the concrete's surface is one of the most advantageous techniques [1]. However, the degrading effect of high temperatures on the adhesive of the bond is one of the main disadvantages for its application. According to Marques [2], Tadeu e Branco [3] and Klamer [4], the mechanical properties, such as resistance and stiffness connection, decrease as a consequence of the adhesive's transition from a glass state to a viscous state at moderately high temperatures, between 60ºC and 82ºC, easily reached in a fire.

This article describes the study of the influence on CFRP laminates bonded to the surface of the concrete by epoxy resin when subjected to different states of tension and increases in temperature with a heating rate of 5ºC/min. This work describes the laboratory resources, the establishment of the experimental model used for double-lap shear tests and the test procedure. The analysis and simulation of the laboratory tests were made via an analytical model built based on the equations in the document of Dai *et al*. [5] and of a finite element model (FEM) through the commercial program *ABAQUS.*

Keywords: epoxy adhesive, CFRP laminate, double-lap shear test, high temperatures, analytical model, numerical model.

2- Experimental study

The studied reinforcing technique consists of adding CFRP laminates, bonded externally to concrete elements through epoxy adhesive. It is intended to measure the connection strength when subjected to shear efforts and under the temperature effect. With this purpose in mind, a laboratory study was developed, in which was carried out a significant number of laboratory tests. The evolution of the relative displacements, the extensions of the CFRP laminate, the surface temperature of the bond and the failure modes are some of the studied parameters in order to better understand of the connection behavior.

2.1 – Characteristics of the materials

The properties of concrete used were experimentally evaluated according to the established in the standard NP EN 12390-3 [6]. The CFRP laminate used had the designation of *S&P Laminates CFK* 150/2000 [7] with longitudinal oriented fibers and the epoxy resin matrix, its modulus of elasticity was estimated 150 GPa. The elasticity modulus adopted to the epoxy adhesive was 8.76 GPa, based on the characterization tests carried out for this resin by Firmo [8]. The summary of the results obtained are presented in tables 1 and 2.

Table 1 – Concrete properties at room temperature.

Características	Concrete (C20/25)
$f_{cm,cube}$(MPA)	28.45
E_{cm}(GPa)	27.39
f_{ctm}(MPa)	2.0

Table 2 – CFRP laminate and epoxy adhesive properties at room temperature.

Properties	CFRP laminate	Epoxy
E_m(GPa)	150	8.76
f_{fd}(MPa)	1000	-

2.2 – Test programme and procedure

To carry out the shear tests a machine Schenck brand was used, with capacity for applying loads up to 500KN and instrumented to get the acquisition of displacements and force applied. The heating of the test specimens was carried out through an attachable furnace of Shumadzu brand, with inside dimensions 1100x280x340 mm^3, with holes in the lower and upper extremes for the application of the load, with heating capacity of up to 200^0C. The evolution of the temperature inside the furnace and in the bond of the test specimens was obtained through K-type thermocouples. The evolution of the extension readings along the instrumented bond length was obtained by TML FLK-6-11-3L type strain gauges for room temperature and type TML BFLA-5-5 for high temperatures. Two displacement transducers (LVDT) were also used and placed in the CFRP laminate's extremes in the bond zone.
The transmission of force in the test specimen was attained through rods of 16 mm diameter steel, embedded in the concrete, with characteristics resistance to traction of 400 MPa.

In the room temperature tests, the load was applied through the displacement control of the shackles' deviation of 0.1 mm/s. In high temperature tests, the application mode of the load through the strength control of the shackles of the test machine led to a practically constant tension state, along the bonded zone, throughout the test time.

In the current work, three levels of static load levels were taken as variables applied to the connection to a constant heating rate of 5ºC/min.

1- Initially, it was tested three test specimens were tested at room temperature (room temperature testing), set to 24.2ºC, to determine the average load of the test specimens' failure, P_u;
2- Secondly, it was tested three groups of test specimens and in each group applied one of the following load levels: 25%, 50% and 75% of P_u, constant over time and submitted to heating rate (high temperature test).

2.3 – Test setup and instrumentation

Each test specimens had two concrete prisms (each one with 350x120x120 mm^3), two CFRP laminates (each one with 600x20x1.4 mm^3), four bonded zones (two in each block and each with 250x20 mm^2) and the armors soaked in concrete through which it transmitted the efforts between the machine straps and the test specimens, as shown in Figure 1.

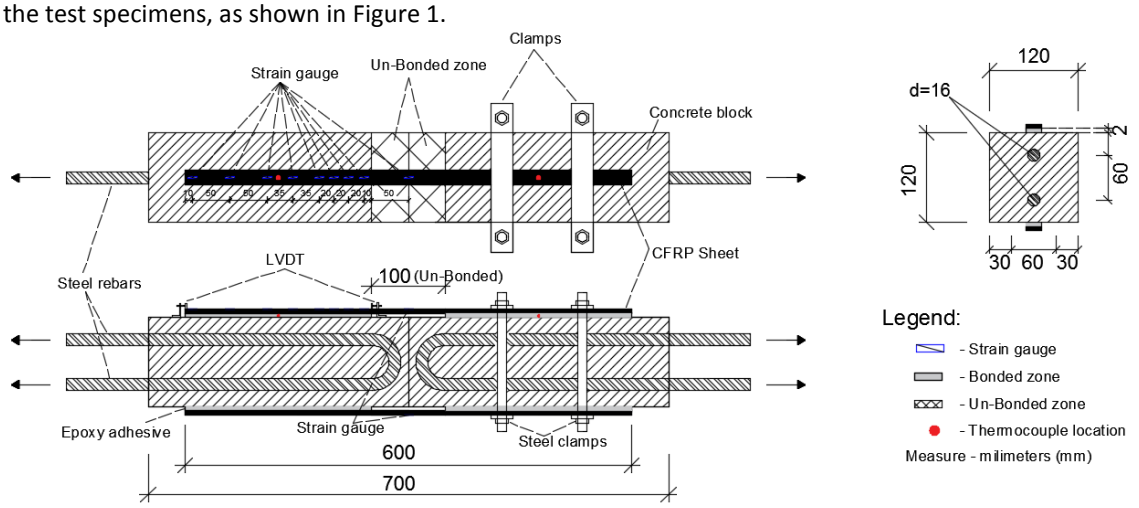

Figure 1 - Double-lap shear test schema.

The preparation of the concrete's surface was made with a needles hammer by chipping the surface (Figure 2 **a)**). The height of the adhesive layer was about 2mm. A thermocouple was placed on the adhesive, centered on the bonded zones of the instrumented CFRP laminate (Figure 2 **b)**), to record the evolution of the adhesive temperature along the testing. The instrumented face is characterized by the application of eight strain gauge**s** distributed in the bonded length to register the extension variations in the connection (Figure 2 **b)**). It was also considered a strain gauge in the symmetry axis of each CFRP laminate of the test specimen (not bonded zone) to control the loading symmetry.

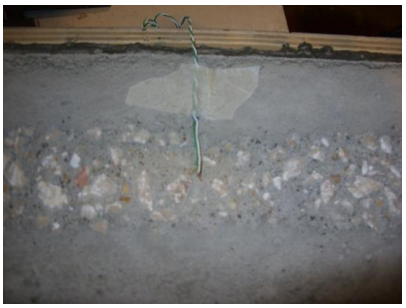

a)

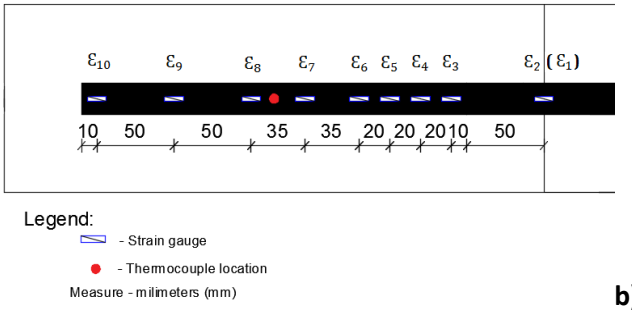

b)

Figure 2 – **a)** Concrete's surface mechanically prepared and thermocouple positioning in the bond area. **b)** Distribution of the strain gauges on the surface of the CFRP laminated.

In the middle of the non-instrumented test specimen was placed an anchoring and protection system with mineral wool to ensure that the failure would occur in the non-instrumented part of the specimen. Figure 3 shows the general appearance of the test specimens ready to be tested at room temperature and at elevated temperatures.

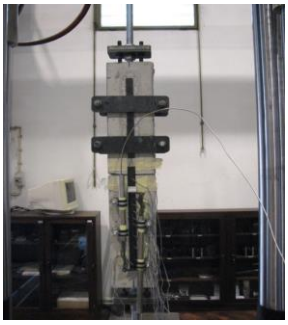

a)

b)

Figure 3 – View of the test set-up: **a)** at room temperature; **b)** at elevated temperature.

3 – Test results

At this point it is presented a summary of the results obtained at the failure time of the tested specimens, by obtaining the data installed in the equipment and instrumentation. The data related with the reading of the strain gages is shown in section 5 together with the analytical and numerical models. For all test results, it was assumed that there was no slip of the test specimens on the clutches of the testing machine.

3.1 – Room temperature testing

It was defined P_u as the average of three obtained results, which is 28.13 KN, as shown in Table 3. In this table, it is also presented the shifts, ways of failure and medium shear stress. The failures occurred suddenly in a blunt way.

Table 3 - Room temperature shear test results.

Test Specimens	Failure load	Failure medium load	Failure displacement	Medium shear stress	Failure mode
	(KN)	(KN)	(mm)	(MPa)	
1º	26.40	28.13	2.21	2.64	Cohesive
2º	30.87		3.01	3.09	Delamination
3º	27.11		2.27	2.71	Cohesive

3.2 – High temperature test

Table 4 presents the results obtained in the high testing's for the shifts of the testing machine, the test time and the registered temperatures in the thermocouples put inside the furnace and in the bond adhesive at the test specimens' failure moment for the 25%, 50% and 75% of P_u.

Table 4 - Obtained results at failure moment for 25%, 50% and 75% of $\boldsymbol{P_u}$.

Test specimens	% Failure médium load	Failure displacement	Time	T1 (bonded zone)	T2 (furnace)	Temperature variation	Failure mode
	(KN)	(mm)	(min)	(ºC)	(ºC)	(ºC)	
1st	25	0.86	59.3	116.9	185.2	68.3	Adhesive
2nd	25	1	63.4	110.5	172.9	62.5	Adhesive
3rd	25	0.98	62.2	118.5	179.1	60.7	Adhesive
1st	50	0.66	32.9	70.6	167.6	97	Adhesive
2nd	50	0.61	30.5	69.3	153.7	84.3	Cohesive/adhesive
3rd	50	0.73	33	74	170.3	96.3	Cohesive/adhesive
1st	75	0.77	26.9	60	147.9	88	Cohesive/adhesive
2nd	-	-	-	-	-	-	-
3rd	75	0.48	27.8	62.1	143.2	81.1	Adhesive

The results revealed that the bigger the tension applied in the test specimens, the lesser the time and respective temperature at which the test specimens failure occurs. The failure modes occurred was mainly by the adhesive and, in some cases, with some concrete pullout together with the adhesive (mixed failure).

4 - Analytical and numerical simulations in a pure shear specimen

At this point, the document presents the properties of the materials considered for modeling, calculation parameters used for the connection simulation throughout the trials at room temperature and at elevated temperatures, as well as the comparison of the results among the analytical and numerical models and the laboratory tests.

4.1 – Numerical model used

Taking advantage of its symmetry, it was modeled ¼ of the test specimens, for simplicity purposes, as shown in Figure 4. This simplification forced the setting restrictions on the shifts that would allow the validity of the assumed symmetry conditions. For modelling 3D solid elements were used to recreate the concrete elements and the CFRP laminates and a contact surface to simulate de adhesive behavior. The epoxy adhesive was modeled by finite elements of CZM's interface (cohesive zone models), based on a cohesive law characterized by parameters that simulate numerically the interfacial fracture of bonded connections.

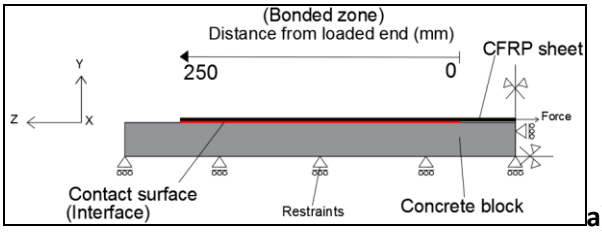

a)

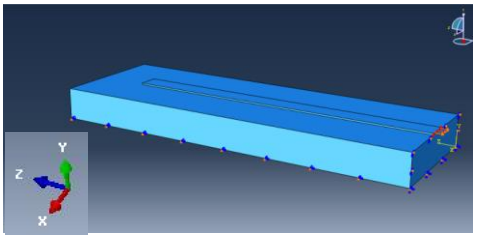

b)

Figure 4 – a) Pure shear specimens (2D). **b)** View of model 3D simulated in a pure shear specimen, in the ABAQUS program.

4.2 – Material parameters set for modelling at room temperature

Table 5 presents the properties and the values considered for the analytical and numerical modelling at room temperature. The epoxy adhesive behavior was modeled through a contact surface with an adhesion-bilinear slipping ration in accordance with Lu *et al* [9].

Table 5 – Material parameters used at room temperature.

Material parameter:	Value	**Material parameter:**	Value
Concrete (linear elastic behavior)		**Epoxy resin (linear elastic behavior)**	
Modulus of elasticity E_c	27.39 GPa	Modulus of elasticity, E_a	8.76 GPa
Poisson's ratio, ν_c	0.2	Poisson's ratio, ν_a	0.35
		Glass transition temperature, $T_{c,a}$	48.5ºC
Laminate CFRP (linear elastic behavior)		**CFRP-to –concrete interface parameters**	
Longitudinal modulus of elasticity , E_l	150 GPa	Maximum shear stress, $\tau_{máx}$	7.38MPa
Glass transition temperature, $T_{c,l}$	141ºC	Fracture energy, G_f	1.45N/mm
Heat transfer coefficient, α_l	[0.7x10^{-6}/ºC]	Initial slip, S_0	0.041mm
		Final slip, S_f	0.391mm
		Shear stiffness, K_t	290.6MPa/mm
		Brittleness index, B_0	10.4mm^{-1}

4.3 – Material parameters set for modelling at high temperatures

To model the test specimens at high temperatures there were considered as basis parameters at room temperature the values in Table 5. As the temperature was rising, the parameters associated with resistance and stiffness of the connection were changing. Among these, the fracture energy (G_f) stands out as well as the brittleness index (B) (adjusts the shape of the tension distribution in the bond length), which are essential to the model calibration. Another aspect taken into account was the decrease of the elasticity module (E_L) of the CFRP laminate to the loss of resistance of the composite matrix. Figure 5 presents these parameters variation based on the equations of the document of Dai *et al* [5].

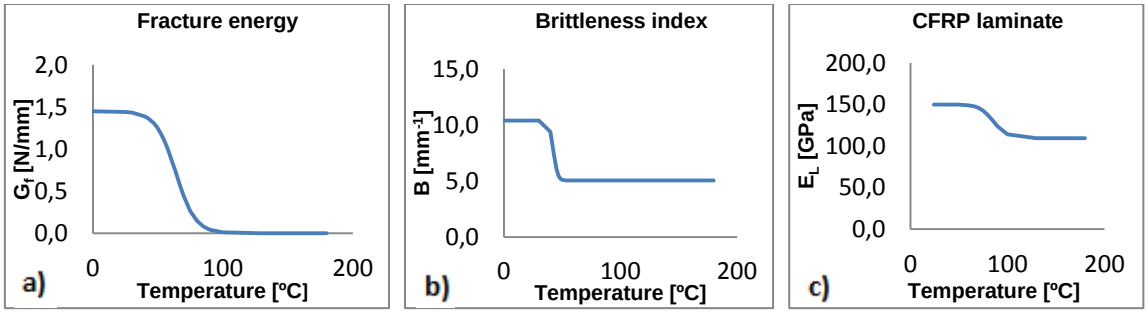

Figure 5 – a) Fracture energy variation. **b)** Brittleness index variation. **c)** Elasticity modulus variation of CFRP laminates.

Figures 6 show the summary of a set of parameters taken into account to simulate the bilinear bond-slip relationship. The bond behavior for a selected range of temperatures, being able to observe the maximum shear stress variation ($\tau_{máx}$) initial slip (s_0) and final slip (s_f), stiffness (K_t) and the fracture energy (G_f) to several load levels. These elements were established in the model in FEM through the introduction of the table data.

T (ºC)	24.2	30	40	50	61	70	80
s_0 (mm)	0.025	0.022	0.023	0.055	0.068	0.102	0.192
$\tau_{máx}$ (MPa)	5.32	4.89	4.05	2.35	1.77	1.06	0.38
Kt (MPa/mm)	211.11	219.36	178.57	42.98	26.05	10.45	1.97
s_f (mm)	0.54	0.59	0.69	1.06	0.96	0.83	0.79
G_f (N/mm)	1.44	1.43	1.39	1.25	0.85	0.44	0.15

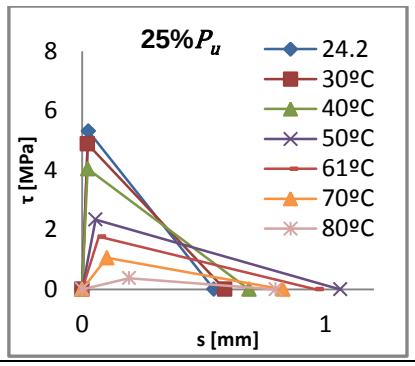

a)

T (ºC)	24.2	30	40	50	61	70
s_0 (mm)	0.059	0.055	0.059	0.133	0.156	0.256
$\tau_{máx}$ (MPa)	7.45	7.34	6.39	3.18	2.15	1.11
Kt (MPa/mm)	125.31	132.28	107.80	24.03	13.73	4.32
s_f (mm)	0.39	0.39	0.43	0.78	0.79	0.79
G_f (N/mm)	1.44	1.43	1.39	1.25	0.85	0.44

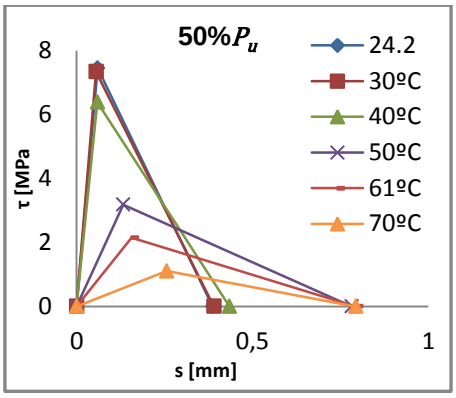

b)

T (ºC)	24.2	30	40	50	61
s_0 (mm)	0.101	0.095	0.104	0.211	0.309
$\tau_{máx}$ (MPa)	7.25	7.27	6.36	3.17	2.15
Kt (MPa/mm)	71.76	76.73	61.20	15.00	6.94
s_f (mm)	0.40	0.39	0.44	0.79	0.79
G_f (N/mm)	1.44	1.43	1.39	1.25	0.85

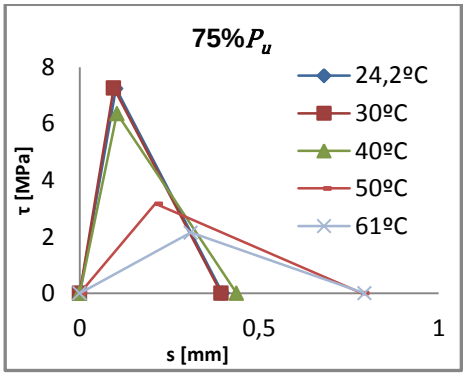

c)

Figure 6 – Bilinear bond–slip relationship at elevated temperature: **a)** 25% $\mathbf{P_u}$; **b)** 50% $\mathbf{P_u}$; **c)** 75% $\mathbf{P_u}$.

Compared to experimental tests, it was found that the temperature for which the theoretical failure occurs was similar for the load levels of 50% and 75% P_u, being 73.5ºC and 64.4ºC respectively, opposing to the load level of 25% P_u, (80ºC). According to Dai *et al.* [5], the equations that originated this analytical model do not account the phenomenon of deformation by viscoelasticity, informing that this phenomenon might have some impact on the results for lighter loads, which might perhaps explain the difference verified for the load of 25% P_u.

5 – Strain distributions in the CFRP laminate - comparison between experimental test, analytical and numerical models

This section presents the graphs obtained for several levels of load, in which was possible to observe the development of the tracing of the curves, which characterize the extensions along the CFRP laminate in the bonded zone for the experimental tests, the analytical model and the numeric model. What concerns the experimental tests, it was assumed a linear variation of values between strain gauges consecutive.

5.1 – Room temperature testing

Figure 7 displays the obtained extensions to apply the three percentages of medium load of failure, being these 25%, 50% and 75% of P_u.

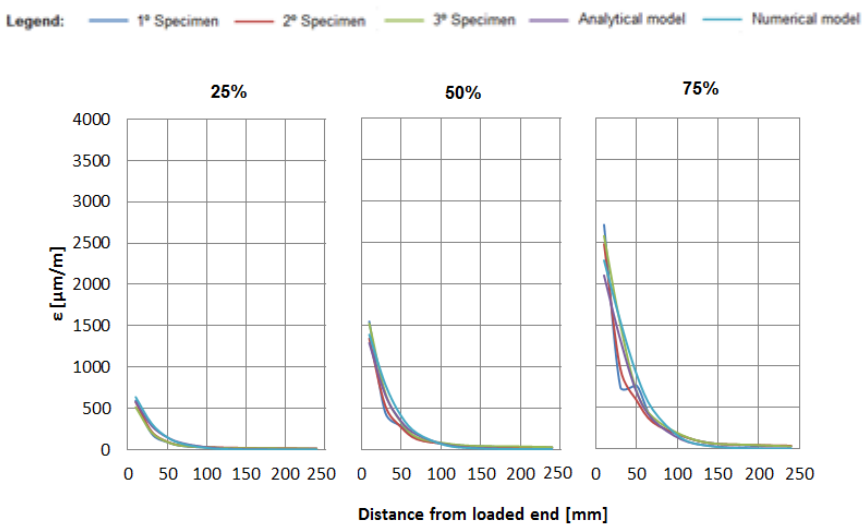

Figure 7 – Comparisons between models and test strain distributions in CFRP laminate at 25%, 50% and 75% of $\boldsymbol{P_{u,}}$, at room temperature.

It was discovered that the analytical and numerical models have a similar development up to 75% $\mathrm{P_{u,}}$. Compared to experimental tests, the analytical and numerical models seem to have less stiffness in the connection from 0 to 100 mm of bond length and more stiffness from 100 mm of bond length of the CFRP laminate, where the extension readings are, in general, bigger and smaller respectively. Just to emphasize that the model was calibrated to allow to have a closer approximation to the values between 0 and 100 mm of bond length, once it was in this length that were developed the tension peaks that influenced the connection sustainability.

5.2 – High temperature test

For the numerical model, it was chosen to simulate the test up to slightly lower temperatures than those of the analytical model, because it was found that above these temperatures the calculation time increased dramatically and the improvement of the results was not significant, which is why was adopted this procedure.

Analyzing Figure 8 **a)** regarding the 25% P_u, it was observed that as the temperature was rising the extensions were increasing. However, for the experimental results it was noticed that in a temperature between 75ºC and 80ºC the extensions started to gradually decrease until it failure the connection. This situation was not verified in the developed analytical and numerical models. In order to simplify the simulation at high temperatures, given the complexity of its behavior, the analytical model was designed up to 85ºC and the numerical model up to 75ºC.

Figure 8 **b)** shows the results of 50% P_u of load being observed that the extensions are similar up to 40ºC. From 40ºC to 55ºC it was verified a slight difference in values, in which the extensions are higher in the analytical and numercial models comparing to the experimental ones. Around 61ºC, the extensions close in and the connection failure occurs at about 70ºC. For simplicity purposes, it was simulated the connection failure in the analytical model up to 73.5ºC and in the numerical model up to 65ºC.

The results achieved at 75% P_u are shown in Figure 8 **c)**, where it was observed that the numerical model presents higher extensions compared to the remaining up to 45ºC. From 45ºC on, these values approximate and keep closer until de connection failure. To simplify the modelling, it was simulated the analytical model up to 64.4ºC and the numerical model up to 55ºC.

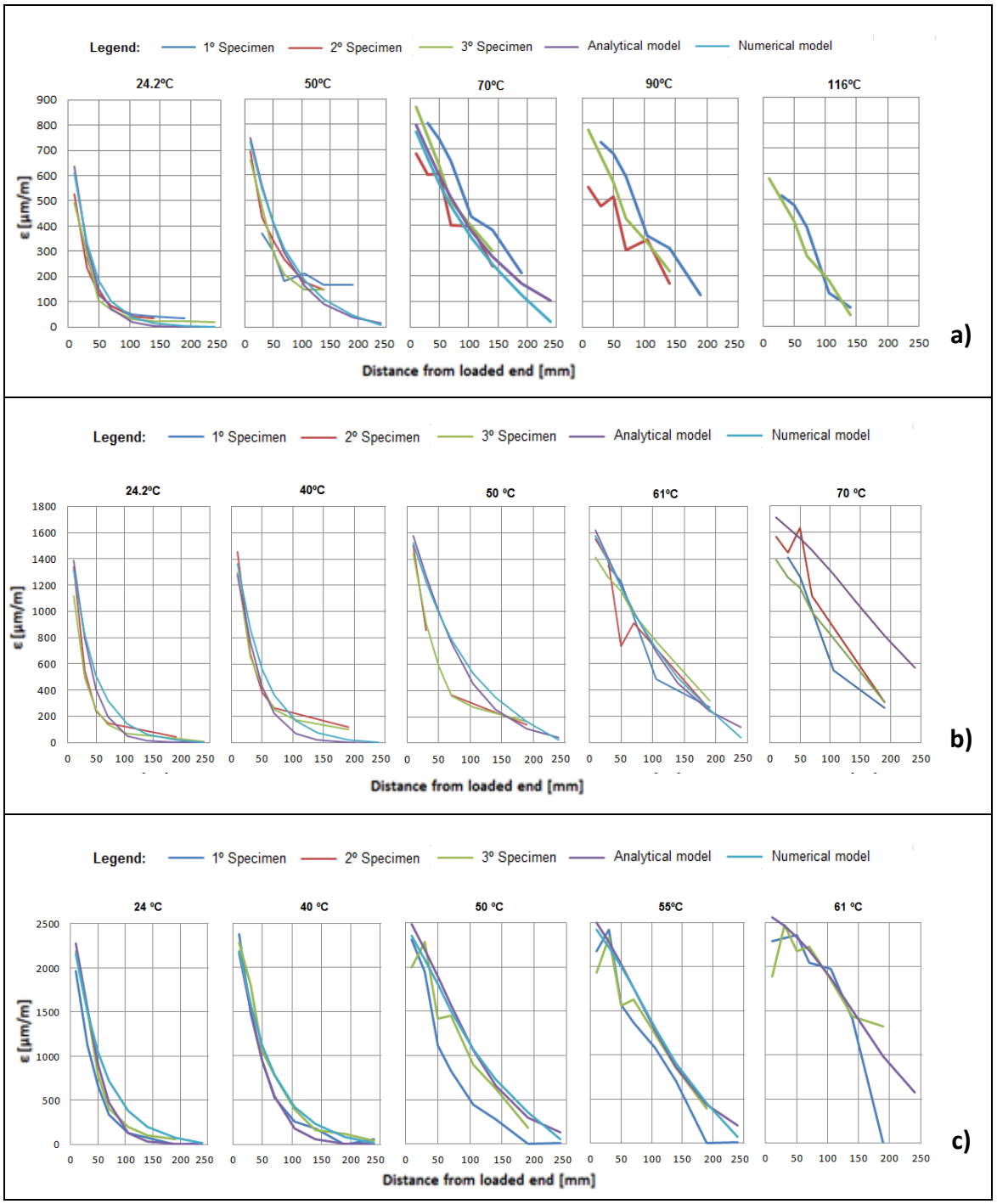

Figure 8 - Extensions in the CFRP laminate: **a)** 25% ,P_u; **b)** 50% P_u.; **c)** 75% P_u.

6 –Shear stress distribution in the bond interface CFRP laminate-concrete - comparisons of results between the analytical and numerical models

Figures 9 display the comparative graphics of shear stress along the bond interface in both analytical and numerical models for the loads and temperatures identified in them.

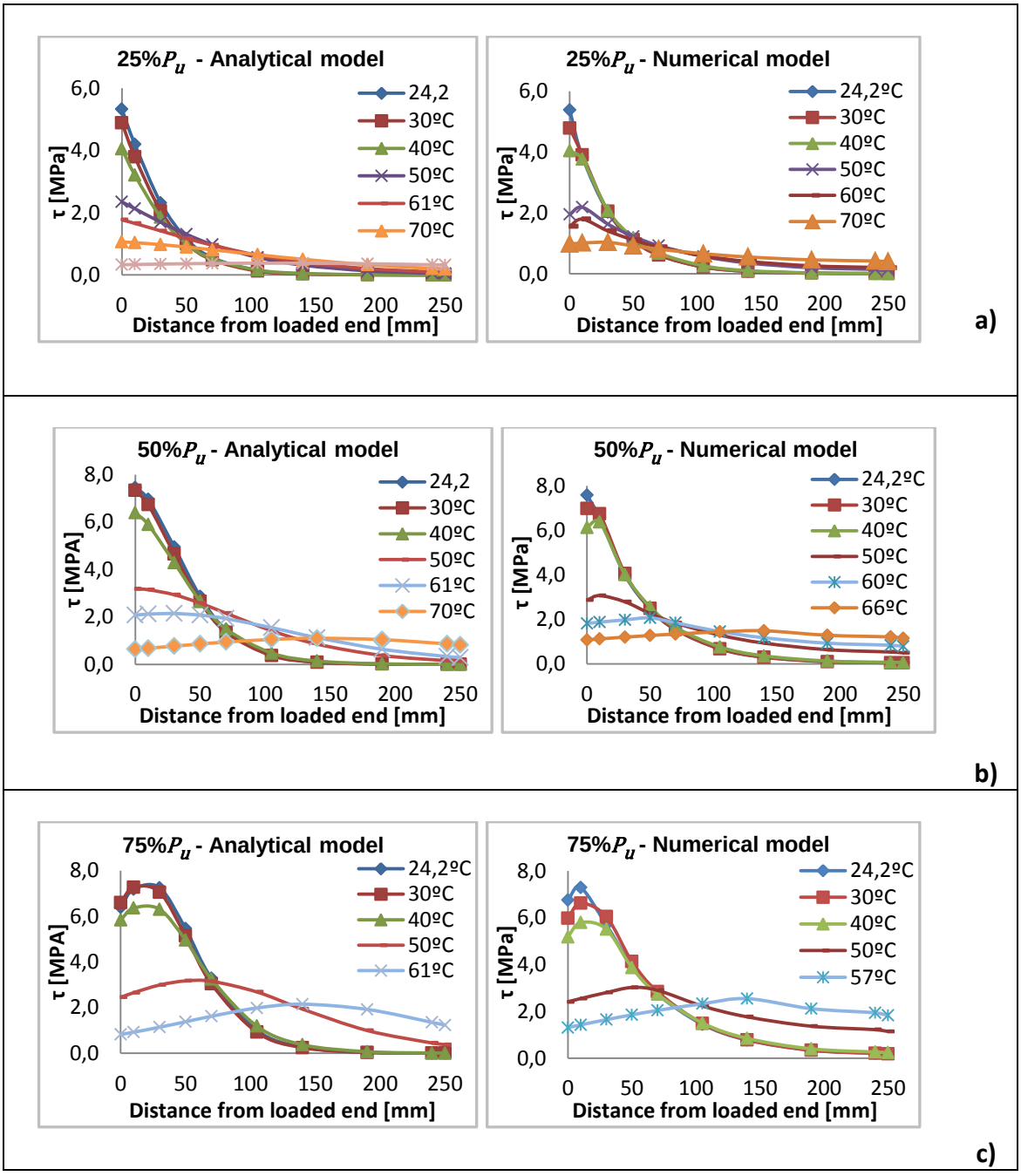

Figure 9 – Comparisons between analytical and numerical models shear stress distributions in CFRP-concrete interface: **a)** 25% P_u **b)** 50% P_u ; **c)** 75% P_u .

After analyzing the Figures shown above, it was verified that the tension distribution in the analytical model is very similar in the numerical model. This affinity is justified by the fact that the numerical model was developed based on the parameters obtained analytical. It should be noted that between 25% - 50% P_u, the peak of shear stress is achieved and that for the temperatures near test specimens failure the tension distribution seems to be almost uniform along the bond length. The maximum temperature reached in the numerical model is slightly lower than the one reached in the analytical model.

7 – Conclusion

The results achieved in the program discussed in this paper demonstrate that the mechanical performance, in terms of adhesion tension, slippage and stiffness, is significantly influenced by temperature increase. As a result, the occurrence of elevated service temperatures should be taken into account, since fire is relevant for the project elaboration.

Preliminary tests, at room temperature, suggest that the resistance of the concrete surface is an element that influences the connection, as observed by several authors in the international literature. Through the developed models, it was found that the maximum shear stress admissible develops in the adjacent zone of the load application. The maximum shear stress admissible in the concrete was 7.38 MPa and 7.54 MPa, for the analytical and numerical models respectively, value from which occurs the failure of the test specimen.

The laboratory tests demonstrate that for the same furnace heating rate of 5ºC/min, the bonded connection sustainability is more vulnerable when subject to higher shear loads, being most relevant for temperatures closer to the glass transition temperature of the adhesive. In the laboratory tests, for the tension states of 25%, 50% and 75% of P_{u}, it was recorded a resistance in the connection up to 115ºC, 71ºC and 61ºC respectively. Given this variation, it can be concluded that the sensitivity of thermomechanical bonding increases considerably to 25% to 50% of P_{u}, about 44ºC, which is lower differential of 50% to 75% % of P_{u}, about 10ºC.

In what concerns the resistance and stiffness parameters of the connection stand at room temperature it stands out the peak tension and the fracture energy that mainly dictate the connection behavior according to what was verified and mentioned by Walander [10]. For the behavior at elevated temperatures, it was found that the set of parameters: peak stress, fracture energy, shape parameter (B), glass transition temperature of the adhesive and the CFRP laminate govern, in a predominant way, the development of bonded connection. Comparing the extensions along the CFRP laminate, it was verified that the analytical model and the numerical model present more proximity among them and, in general, with the obtained values in laboratory, mainly for the 50% and 75% of $\mathrm{P_u}$. For the load level of 25% P_{u} the reached temperature in the failure was considerably lower for the analytical and numerical models, for what they are more conservative in this aspect. According to Dai *et al* [5], this fact can be explained by the fact that the viscoelasticity deformation was not considered in the analytical model, which may have some impact on the results for lighter loads applied.

References

1. Juvandes, L. *"Reforço e Reabilitação de Estruturas de Betão usando Materiais Compósitos de CFRP",* PhD Thesis, Civil Engineering, University of Porto, 1999.

2. Marques, A. *"Introdução aos materiais poliméricos",* Construction and Building Material. - Thesis for the degree of licenciate of Engineering Mechanics, University of Porto, 1982.

3. Tadeu, A. e Branco, F. *"Shear Tests of Steel Plates Epoxy-Bonded to Concrete under Temperature", Journal of Materials in Civil Engineering*, ASCE, Vol.12, nº1, p. 74-80, 2000.

4. Klamer, E. *"The influence of temperature on concrete structures strengthened with externally bonded CFRP",* Research Report, Eindhfurnace University of Techonology, Netherlands, 2006.

5. Dai, J., Gao, W. e Dai, J. *"Bond-slip model for laminates externally bonded to concrete at elevated temperatures*", *Journal of Composites for Construction,* p. 33, 2012.

6. 12390-3, NP EN. "*Ensaios de betão endurecido, Parte 3: Resistência à compressão de provetes de ensaio".* Lisbon, IPQ, 2009.

7. *S. C. R. Company, "Design Guide Line for S&P FRP Systems", Brunnen, Switzerland, p.58., 2006.*

8. Firmo, J. *"Comportamento ao fogo de vigas de betão armado reforçadas à flexão com laminados de fibras de carbono"*, Master's Degree in Civil Engineering, Instituto Superior Técnico - technical University of Lisbon, 2010.

9. Lu, X., et al., et al. *"Bond-slip models for FRP sheets/plates bonded to concrete",* Engineering Structures, Vol. 27,pp. 920-937, 2005b.

10. Walander, Tomas. *"Cohesive modelling of the temperature dependence of epoxy based adhesives in Mode I and Mode II loading"*, Departament of Applied Mechanics, Thesis for the degree of licenciate of engineering en Aplllied Mechanics, Chalmers university of Techonology, Gothenburg, Sweden, 2013.